Insights into the cytotoxic activity of the phosphane copper(I) complex [Cu(thp)4][PF6]

Thermodynamic stability and structure in aqueous solution of the $[Cu(PTA)_4]^+$ complex (PTA = aminophosphine 1,3,5-triaza-7-phosphaadamantane)

Martina Quaretti[a], Marina Porchia[b], Francesco Tisato[b], Angela Trapananti[c], Giuliana Aquilanti[d], Marko Damjanovic[e], Luciano Marchiò[a], Marco Giorgetti[f,], Matteo Tegoni[a,*]*

[a] Department of Chemistry, Life Science, and Environmental Sustainability, University of Parma, Parco Area delle Scienze 11A, 43124 Parma, Italy.

[b] CNR-ICMATE, Corso Stati Uniti 4, 35127 Padova, Italy.

[c] School of Science and Technology - Physics Division, University of Camerino, Via Madonna delle Carceri; 62032 Camerino, Italy

[d] ELETTRA Sincrotrone Trieste, ss 14, km 163.5, 34149 Basovizza, Trieste, Italy

[e] Anorganisch-Chemisches Institut, University of Heidelberg, Im Neuenheimer Feld 27, Heidelberg, DE 69120, Germany.

[f] Department of Industrial Chemistry, University of Bologna, Viale del Risorgimento 4, 40136 Bologna, Italy.

KEYWORDS

Copper(I); PTA; XAS; Metallochromic indicators; Speciation; Formation Equilibria

ABSTRACT

The chemistry of copper(I) with water-soluble phosphine is an emergent area of study which has the objective of finding ligands that stabilize copper in its lower oxidation state. Cu(I) has been found relevant in the mechanism of copper transports into cells, and the accessibility of this oxidation state has implications in oxidative stress processes. For these reasons the possibility to deal with stable, water soluble copper(I) is an attractive approach for devising new biologically relevant metal-based drugs and chelating agents. Here we present the XAS and UV-visible spectrophotometric study of the $[Cu(PTA)_4]BF_4$ complex. In particular, we have studied the stability of the $[Cu(PTA)_n]^+$ species (n = 2-4) in aqueous medium, and their speciation as a function of the total $[Cu(PTA)_4]BF_4$ concentration by means of competitive UV-visible spectrophotometric titrations using the metallochromic indicators BCA^{2-} and i-BCS^{2-}. Also, the structure in solution of the Cu(I)/PTA species and the nature of the first coordination sphere of the metal were studied by X-ray absorption spectroscopy. Both techniques allowed to study samples with total $[Cu(PTA)_4]BF_4$ concentration down to 68-74 μM, possibly relevant for biological applications. Overall, our data suggest that the $[Cu(PTA)_n]^+$ species are stable in solution, among which $[Cu(PTA)_2]^+$ has a remarkable thermodynamic stability. The tendency of this last complex to form adducts with N-donor ligands is demonstrated by the spectrophotometric data. The biological relevance of PTA towards Cu(I), especially in terms of chemotreatments and chelation therapy, is discussed on the basis of the speciation model the Cu(I)/PTA system.

HIGHLIGHTS

- $[Cu(PTA)_4]^+$ undergoes PTA dissociation at concentration lower than 10 mM
- The $[Cu(PTA)_2]^+$ fragment has a remarkable stability in aqueous solution
- $[Cu(PTA)_2]^+$ forms very stable adducts with nitrogen-containing ligands
- The $[Cu(PTA)_2]^+$ fragment is possibly the biologically relevant species

GRAPHICAL ABSTRACT

The speciation of the Cu(I)/PTA system has been studied in aqueous solution. XAS data and UV-visible spectrophotometric titrations allowed to determine the thermodynamic stability of the $[Cu(PTA)_n]^+$ species along with their structure in solution. Experimental evidences show a remarkable stability of the $[Cu(PTA)_2]^+$ species and its tendency to form stable complexes with nitrogen co-ligands.

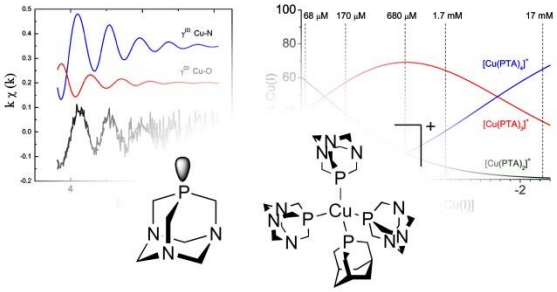

1. Introduction

The coordination chemistry of water-soluble aminophosphine 1,3,5-triaza-7-phosphaadamantane (PTA, Scheme 1A) with transition metals has been a flourishing research area in the last two decades.[1–3] The ability of PTA to solubilize transition metal complexes in aqueous phase made these compounds ideal candidates in the biphasic or aqueous phase homogenous catalysis and, more recently, for medicinal chemistry applications.[2,3] An illustrative example of this dual action is represented by mixed ruthenium complexes of the type $[(Cp^*)RuCl(PTA)_2]$ (Cp^* = cyclopentadienyl and substituted-cyclopentadienyl ligands), reported as regioselective catalysts for hydrogenation of ketones in aqueous biphasic conditions,[4,5] and as potential cytotoxic agents toward murine TS/A adenocarcinoma cell lines.[4,6] Related [(μ^6-arene)$RuCl_2(PTA)$] compounds, named RAPTA, showed peculiar selectivity towards metastatic tumors.[7] In RAPTA, PTA is reported both to convey good water solubility which is a critical issue for therapeutic application, and to impart good thermodynamic stability to the overall system. Tumor uptake and selectivity are then tuned by modification of the lipophilic character of the arene moiety or by replacing labile chloride(s) with neutral donors.[8]

In search for hydrophilic Cu(I)-based antitumor agents, our research group described recently the cytotoxic potential of $[Cu(P)_4]^+$-type compounds (P = hydrophilic tertiary phosphine).[9,10] Among the complexes of this class, the tetrahedrally-arranged Cu(I) complex $[Cu(PTA)_4]^+$ (Scheme 1) was firstly synthetized and characterized a decade ago by Kirillov and coworkers.[11,12] Although $[Cu(PTA)_4]^+$ did not show the best efficiency in terms of cytotoxicity in *in vitro* experiments (IC_{50} in the low micromolar range) among the series of investigated $[Cu(P)_4]^+$ complexes, its distinctive biological features somehow resembles those shown by RAPTA derivatives.[13] In particular, it exhibits rapid and exponential uptake in implanted EMT-6 cells, with more than 8.0 % association at 2 h during in *in vivo* experiments

using the radiolabeled $[^{64}Cu(PTA)_4]^+$ species.[13] The moderate *in vitro* cytotoxicity of $[Cu(PTA)_4]^+$ parallels with the behavior observed for RAPTA compounds; however, both PTA-containing copper and ruthenium compounds show pronounced anti-metastatic activity (Ru),[14,15] and anti-angiogenic and anti-malarial activities (Cu).[16,17]

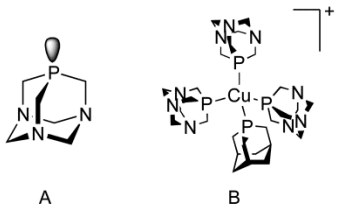

Scheme 1. A: Representation of the PTA ligand; B: representation of the $[Cu(PTA)_4]^+$ cation.

Since free PTA was found to exert no cytotoxic, no anti-angiogenic and no anti-malarial effects, it is likely that the biological properties induced by $[Cu(PTA)_4]^+$ should be the result of a direct interaction of the metal with specific target substrates such as proteins. From a molecular point of view, it is hard to presume a direct metal-substrate interaction of the coordinative saturated tetrahedral complex, unless dissociation of one or more phosphines in solution is taken into account. While tetrahedral coordination of copper(I) to four PTA molecules was found in the solid state and in the solution state at elevated concentrations,[9,11] coordinative unsaturated $[Cu(PTA)_2]^+$ and $[Cu(PTA)_3]^+$ species were detected under electrospray ionization mass spectrometry (ESI-MS) conditions at micromolar concentrations.[18] Since perturbation of the analytes composition cannot be ruled out *a priori* due to the application of high voltages at the spray capillary, we decided to investigate the speciation of $[Cu(PTA)_4]^+$ dissolved in water at different concentrations with other physico-chemical techniques.

Recently a study on the thermodynamics of formation of $[Cu(PTA)_n]^+$ species (n = 1-4) in 1 M NaCl aqueous solution by means of potentiometric, spectrophotometric and microcalorimetric methods has been reported.[19] In this study we were able to determine the stability of the various Cu(I)/PTA species in aqueous environment under high Cl^- concentration, the latter used to stabilize copper in the +1 oxidation state. The drawback of this approach is that the high concentration of chloride ions promoted the formation of mixed Cu(I)/Cl^-/PTA species such as [CuCl(PTA)] or $[CuCl(PTA)_2]$ species which made more complex the speciation of this system.[19]

The high Cl^- concentration acted as a *self-medium* condition, with the result that the formation constants of the complexes should be considered *conditional* rather than *thermodynamic* stability constants. Therefore, the stability constants of the species $[Cu(PTA)_n]^+$ complexes (n = 1-4) in a chloride-free medium could be only estimated, resulting into *ca*. 5 log units higher than those determined in 1 M Cl^- conditions. Although these values are in agreement with those expected for a medium lacking the competing ligands, no experimental insights were provided for these conditions.[19]

In this follow-up paper we present the results of a spectroscopic and thermodynamic study of the stability of $[Cu(PTA)_4]^+$ system in aqueous, chloride-free environment. Our purpose was to move one step forward into the elucidation of the speciation and stability of these Cu(I)/phosphine complexes in aqueous media and, possibly, to confirm or refuse the speciation expected in the absence of chloride ions. Here we have used the excellent selectivity for the atomic species of the extended portion of the X-ray Absorption Spectroscopy (XAS) probe to gain insight on the average coordination environment of Cu(I) in $[Cu(PTA)_4]^+$ samples between 68 μM and 17 mM concentration. With these data in hands, we have used metallochromic

competing ligands for Cu(I) to determine the stability of the predominant species in aqueous HEPES buffer (100 mM, pH 7.4) solution. This approach is similar to that we used recently for the study of the stability of the $[Cu(thp)_n]^+$ species (thp = tris(hydroxymethyl)phosphine).[20] The thermodynamic data were compared to those of $[Cu(PTA)_4]^+$ in the presence of chloride ions, and analyzed in light of previously reported mass spectrometric data. The results are discussed in view of the reported biological functions of the $[Cu(PTA)_n]^+$ fragments.

2. Experimental section

2.1 Materials and methods

Commercially available chemicals were of high purity grade and used as received. The reagents 4,4'-dicarboxy-2,2'-biquinoline disodium salt ($BCA(Na)_2$), bathocuproinedisulfonic acid disodium salt ($i\text{-}BCS(Na)_2$), microcristalline cellulose powder, L-phenylalanine, and sodium ascorbate were obtained from Sigma-Aldrich. The Cu(I) precursor complex $[Cu(CH_3CN)_4]BF_4$ was prepared by reaction of $[Cu(H_2O)_6](BF_4)_2$ with metallic copper in acetonitrile, as reported in the literature.[21] PTA and the complex $[Cu(PTA)_4]BF_4$ were synthesized according to published methods.[11,12]

2.2 XAS Data Collection

XAS spectra at the Cu K-edge have been recorded at GILDA-BM08 beamline (now LISA) of the European Synchrotron Radiation Facility, ESRF (Grenoble, France).[22] The storage ring was operated at 6 GeV in uniform mode with a maximum electron current of 200 mA. The white beam from the bending magnet source was monochromatized using a fixed-exit double-crystal

Si(111) monochromator. The second crystal was sagittally curved to focus the beam in the horizontal plane and dynamical focusing was used to keep the beam size on the focal point constant throughout a full energy scan. Harmonics were rejected using two Pd-coated mirrors working at an incidence angle of 3.6 mrad. Aqueous solutions of 17 mM, 1.7 mM, 680 μM, 170 μM and 68 μM of have been measured using a cell for liquids with Mylar windows. XAS spectra in fluorescence mode were collected at room temperature using a 13-element hyper-pure Ge detector (manufactured by ORTEC) equipped with fast digital electronics (XIA 4C/4T Digital X-ray Processing (DXP)). The energy discriminating Ge detector was placed at 90 degrees to the incident x-ray beam to minimize the contribution of elastic scattering in the fluorescence spectrum. A solid sample of $[Cu(PTA)_4]BF_4$ has been recorded in transmission mode. The solid sample has been prepared by mixing 51 mg of $[Cu(PTA)_4]BF_4$ with 158 mg of microcrystalline cellulose powder to obtain a suitable absorption length and then pressed to 3 tons to obtain a pellet. The 17 mM $[Cu(PTA)_4]BF_4$ mother solution of for XAS measurements has been prepared by dissolving 13.8 mg of $[Cu(PTA)_4]BF_4$ in 1000 μL in Millipore UPP water. Solutions of 1.7 mM, 680 μM, 170 μM and 68 μM have been prepared by dilution of the mother solution. Three to four scans were collected for each solution, using a fresh samples each time. This protocol for the data acquisition was necessary especially for the highest concentrated samples, in order to avoid any sample alteration after the exposure to the X-ray beam.

XAS spectra were measured at room temperature, up to 1100 eV above the edge with 10 seconds acquisition time/point. The energy step was chosen to be 0.5 eV in the edge region; 1 eV after the edge, and 2 and 4 in the extended range. Before and after each absorption measurement, a reference spectrum of Cu metal foil (for which the edge energy is 8980.3 eV, corresponding to

the first inflection point) was collected to check for energy drifts of the monochromator. XAS spectra were measured at room temperature.

2.3 XANES and EXAFS Analysis

X-ray Absorption Spectroscopy spectra were deglitched and calibrated using the Athena program.[23] The pre-edge background was removed by subtraction of a linear function extrapolated from the pre-edge region, and the X-Ray Absorption Near Edge Structure (XANES) spectra were normalized at the unity by extrapolation of the atomic background as it comes out from the EXAFS analysis. The post-edge background has been modeled using a polynomial function. The analysis of the edge portion of the XAS spectrum, *i.e.* the 1s-4p transition in Cu(I) complexes, has been carried out by extrapolating the data using an arc-tangent function. The obtained peaks were fitted with the pseudo-Voigt function.[20]

The EXAFS analysis has been performed by using the GNXAS package that takes into account Multiple Scattering (MS) theory.[24] The method is based on the decomposition of the EXAFS signals into a sum of several contributions, that are the n-body terms. It allows the direct comparison of the raw experimental data with a model theoretical signal. The procedure avoids any filtering of the data and allows a statistical analysis of the results. The theoretical signal is calculated *ab-initio* and contains the relevant two-body $\gamma^{(2)}$, the three-body $\gamma^{(3)}$ and the four body $\gamma^{(4)}$ multiple scattering (MS) terms.[25] The two-body terms are associated with pairs of atoms and probe their distances and variances. The three-body terms are associated with triplets of atoms and probe angles, bond-bond and bond-angle correlations. If useful, a single effective MS signal $\eta^{(3)}$ that includes both $\gamma^{(2)}$ and the $\gamma^{(3)}$ contributions can be used for the shells beyond the second one by using the same three-atom coordinates both for the two-atom and the three-atom

contributions. The four-body terms are associated to chains of 4 atoms, and probe distances and angles in between, and bond-bond, and bond-angle correlations. In this application the contribution from four-body terms has been checked out, but it was found to be negligible.

Data analysis is performed by minimizing a χ^2-like residual function that compares the theoretical signal, $\alpha_{mod}(E)$, to the experimental one, $\alpha_{exp}(E)$. The phase shifts for the photoabsorber and backscatterer atoms were calculated *ab-initio* from the solid structure of $[Cu(PTA)_4]BF_4$ according to the muffin-tin approximation and allowing 10-15% overlap between the muffin-tin spheres.[9] The Hedin-Lundqvist complex potential was used for the exchange-correlation potential of the excited state.[26] The core hole lifetime, Γc, was fixed to the tabulated value and included in the phase shift calculation.[27] The experimental resolution used in the fitting analysis was about 1 eV, in agreement with the stated value for the beamline used. The relevant E_0's values were found to be displaced by several eV with respect to the edge inflection point.

The observed values for the amplitude reduction factor were in the 0.76(5) and 0.86(8) range, whereas the E_0's values have been found to be displaced only few eV with respect to the edge inflection point. The total number of parameters taken into account in the fitting procedure (including the structural and non-structural terms E_0, S_0^2 and the experimental resolution) were 13, whereas the number of floating variable (fitting) was found to be 11. Besides, it is worth mentioning that in all cases the number of fitting parameters has not exceeded the estimated number of independent data points ($N_{ind} = (2 \cdot \delta k \cdot \delta R/\pi)+2$), ensuring that the fit is well determined, thus confirming the reliability of the present minimization.

2.4 Potentiometric measurements

The glass-electrode potentiometric titrations of PTA and of $[Cu(PTA)_4]BF_4$ were carried out in aqueous solution at $T = 298.2 \pm 0.1$ K and $I = 0.1$ M (KCl) under a N_2 stream, using 5 mL samples. The potentiometric titrations were carried out using an automatic system consisting in a Metrohm Dosimat 665 automatic dosimeter (for titrant addition) and an Orion 720A pH-meter provided with a Hamilton combined glass electrode (for pH measurements). The system was controlled by a PC to monitor the attainment of the equilibrium through pH measurements *vs*. time, and the addition of titrant aliquots. The Hamilton combined glass electrode (P/N 238000) was calibrated in terms of $[H^+]$ by titrating HCl solutions with KOH (hereafter pH = -log $[H^+]$),[28] and the pK_w value resulted to be 13.77(1). The protonation constants of PTA were determined by alkalimetric titration of 3 samples (3.5 – 4.5 mM). The protonation constants of $[Cu(PTA)_4]^+$ were determined by alkalimetric titration of 3 samples (1.4 – 1.9 mM of $[Cu(PTA)_4]BF_4$). The pH range explored was *ca.* 2 – 11; no proton dissociation processes attributable to metal hydrolysis were observed. All samples were prepared by weight of the pure solids, and dissolved in freshly prepared, N_2 fluxed, doubly distilled water.

2.5 UV-visible spectrophotometric studies

The spectrophotometric titrations were carried out in aqueous buffer HEPES solutions (100 mM, pH 7.4) to prevent possible variation of the pH due to the addition of metallochromic indicators (weak bases) and to maintain constant the ionic strength. The aqueous buffer medium was prepared by suspending solid HEPES in freshly boiled doubly distilled water. Addition of small aliquots of a concentrated NaOH aqueous solution resulted in the dissolution of solid HEPES. The pH was then corrected to 7.4 by addition of further aliquots of NaOH. The buffer medium was passed through a 0.45 μm nylon filter, transferred into an air-free Schlenk vessel,

and deoxygenated by purge with a N_2 stream before storage. The pH was checked every 2-3 days and corrected with small quantities of NaOH or solid HEPES where required.

All sample solutions were prepared using freshly N_2-fluxed (at least 5 min) HEPES buffer medium, which was transferred into the cuvette and added with solid sodium ascorbate (to obtain a 10 mM concentration) prior of reactant mixing. The UV-visible spectra were collected using a Thermo Evolution 260 Bio spectrophotometer provided with a Peltier thermostatting device, and Teflon-sealed quartz cuvettes (1 cm path length). All solutions used for spectrophotometric analyses were prepared using nitrogen-saturated 100 mM aqueous HEPES buffer (pH 7.4), or high purity water.

Stock solutions (40 mM) of the metallochromic indicators i-BCS$(Na)_2$ and BCA$(Na)_2$ were prepared by dissolving proper amounts of the solid salts in D_2O (700 µl volume). The concentration of these solutions was determined by ^1H NMR using a solution of high purity L-phenylalanine in D_2O (prepared by weight) as an external standard. Titrant solutions of i-BCS$(Na)_2$ and BCA$(Na)_2$ ($C_{i\text{-}BCS}$ = 1.34 mM, C_{BCA} = 1.60 mM) were prepared by dilution of the stock solutions in aqueous HEPES buffer (100 mM, pH 7.4). The stock solution of $[Cu(CH_3CN)_4]BF_4$ (C_{Cu} = 1.64 mM) was prepared by weight in acetonitrile. The stock solution of $[Cu(PTA)_4]BF_4$ (C_{Cu} = 0.64 mM) was prepared by weight in doubly distilled water.

Titrand sample solutions of $[Cu(CH_3CN)_4]BF_4$ were prepared directly in the quartz cuvette: 2.4 ml of nitrogen bubbled HEPES buffer were added with *ca*. 5.1 mg of sodium ascorbate to obtain a 10 mM ascorbate concentration. The stock solution of $[Cu(CH_3CN)_4]BF_4$ was added (200 µl) to obtain a final formal *ca*. 126 µM concentration of $[Cu(CH_3CN)_4]BF_4$. The solutions were titrated with either i-BCS^{2-} or BCA^{2-} (up to a Cu(I):ligand = 1:2.4).

Titrand sample solutions of $[Cu(PTA)_4]BF_4$ were prepared directly in the quartz cuvette: 2.3 ml of nitrogen bubbled HEPES buffer were added with *ca*. 5.1 mg of sodium ascorbate to obtain a 10 mM ascorbate concentration. The stock solution of $[Cu(PTA)_4]BF_4$ was added (300 µl) to obtain a final formal *ca*. 74 µM concentration of $[Cu(PTA)_4]BF_4$. The solutions were titrated with either i-BCS^{2-} (up to Cu(I):i-BCS^{2-} = 1:4.1), or BCA^{2-} (up to Cu(I):BCA^{2-} = 1:2.4).

Titrand sample solutions of $[Cu(CH_3CN)_4]BF_4$ in the presence of 2 eq. of BCA^{2-} were prepared directly in the quartz cuvette: 2.24 ml of nitrogen bubbled HEPES buffer were added with *ca*. 5.1 mg of sodium ascorbate to obtain a 10 mM ascorbate concentration. The stock solution of $[Cu(CH_3CN)_4]BF_4$ (200 µl) was added with 160 µL of the $BCA(Na)_2$ solution (C_{BCA} = 1.60 mM) to obtain final formal concentrations of 126 µM and 256 µM for $[Cu(CH_3CN)_4]BF_4$ and BCA^{2-}, respectively. The solution was titrated with i-BCS^{2-} up to Cu(I):i-BCS^{2-} = 1:3.0.

Titrand sample solutions of $[Cu(PTA)_4]BF_4$ in the presence of 1.3 eq. of BCA^{2-} were prepared directly in the quartz cuvette: 2.145 ml of nitrogen bubbled HEPES buffer were added with *ca*. 5.1 mg of sodium ascorbate to obtain a 10 mM ascorbate concentration. The stock solution of $[Cu(PTA)_4]BF_4$ was added (300 µl) toghether with 155 µL of the $BCA(Na)_2$ solution (C_{BCA} = 1.60 mM) to obtain final formal concentrations of 74 µM and 93 µM for $[Cu(PTA)_4]BF_4$ and BCA^{2-}, respectively. The solutions were titrated with i-BCS^{2-} up to Cu(I):i-BCS^{2-} = 1:2.6.

In all samples containing $[Cu(CH_3CN)_4]BF_4$, the amount of acetonitrile did not exceed 7 % total volume. All titrations were performed in triplicate.

2.6 Potentiometric and spectrophotometric data treatment

Spectral data were treated using the software HyperQuad 2006 in order to calculate the log β values of the of the complex formation equilibria operating in the examined system and, where required, the molar absorbance of the colored species present in solution.[29] Spectrophotometric data from different titrations of the same system (replicates) were treated together. Water was considered as self-medium. The formation constant ($\log \beta_2 = 19.8$) of $[Cu(i\text{-}BCS)_2]^{3-}$ was used as the only fixed parameter (see below).[30–33] Acetonitrile as a possible competing ligand was taking into account through the formation constants in aqueous solution of the $[Cu(CH_3CN)_n]^+$ (n=1-3) complexes,[34] resulting into a negligible contribution. All molar spectra of the complex species of $i\text{-}BCS^{2-}$ and BCA^{2-} were calculated as refined parameters. The molar spectra of the BCA^{2-} and $i\text{-}BCS^{2-}$ ligands were also taken into account as fixed parameters, although their contribution resulted negligible at the concentrations used and in the spectral range examined.

The potentiometric data were treated with the HyperQuad 2006 program.[29] Titrations related to the same system (replicates) were treated together in the calculations. The distribution diagrams were calculated using the HySS 2009 software.[35]

3. Results and discussion

3.1 XAS studies - Analysis of the pre-edge structures and XANES

We first studied the average coordination environment of Cu(I) in aqueous $[Cu(PTA)_4]^+$ samples using XAS techniques. Since in this study we also aimed to determine the stability of

the $[Cu(PTA)_n]^+$ complexes, XAS data were collected in particular on samples at low (*ca*. 100 μM) concentrations, which are those used for the study of complex formation equilibria.

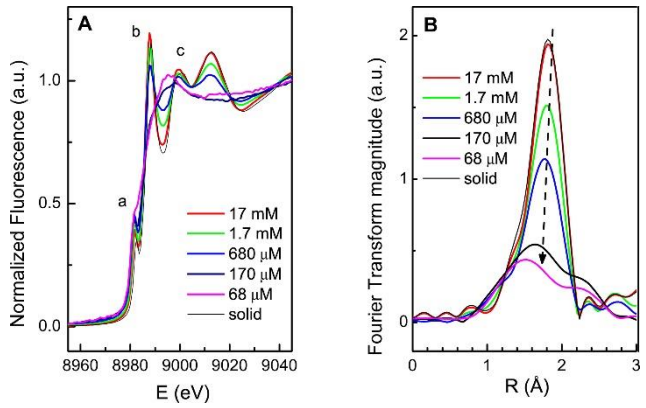

Fig. 1. A: Experimental and normalized XANES spectra taken at the Cu K-edge (8979 eV) of $[Cu(PTA)_4]BF_4$ at different concentrations. 1s-4p transition (feature a), main edge (feature b) and multiple scattering resonances (feature c) regions are indicated. B: Experimental FT curves of the corresponding EXAFS signals of $[Cu(PTA)_4]BF_4$ at different concentrations.

Fig. 1A displays the normalized XANES traces recorded at different concentrations of $[Cu(PTA)_4]BF_4$ in water, from 17 mM down to 68 μM. Acquisition of XAS data on such a dilution level is very challenging and unusual. Nevertheless, the low-energy photoelectron probe is certainly suitable as spectra change dramatically in both intensity and shape of the main features. Cu K-edge XANES spectra are well studied.[36,37] Structure contributing peaks on and above the broad absorption of the rising edge depends strongly to both the oxidation state and local structure of Cu. The feature with the lowest energy (pre-edge) is typically the dipole forbidden but quadrupole allowed 1s-3d transition. The intensity of this transition is sensitive both to the ligation symmetry of the absorber and to the covalence of the metal-ligand bond. This transition gains additional intensity in a non-centrosymmetric environment through 3d/4p orbital

mixing, it can be observed for Cu(II) species, is absent in Cu(I) complexes and can usually be found around 8981 eV for Cu(III) complexes.[38] Its absence in the spectra of Fig. 1A confirms the Cu(I) oxidation state in all investigated solutions. A well-known feature appears as a shoulder along the rising edge before the principal edge maximum (Fig. 1 feature a). This has been assigned as the 1s-4p transition.[38,39] For Cu(I) this rising edge shoulder occurs at about 8981-8984 eV, while for Cu(II) a shift to higher energies is expected (ca. 8987 eV). Also, in the case of Cu(I) the transition shows the highest intensity for linear two-coordinated complexes and becomes less intense and broadened as the coordination number increases and/or the symmetry is lowered.[38] The progressive increase of the 1s-4p electronic transition upon dilution (Fig. 1A) clearly indicates a Cu-P coordination number decreasing. An analysis of the 1s-4p transition was carried out by extrapolation of the normalized XANES data using an arc-tangent function. The obtained peaks were fitted with the pseudo-Voigt function. Example of this data treatment is available as Supporting Information (Fig. S1). The units of all the peak intensities are given in normalized area units (nau) and they have been indicated in Table 1. Table 1 also contains the centroid positions for the corresponding peaks. The centroid of the peak is seen the same in all spectra, once again demonstrating that the Cu charge retains upon dilution.

Further, an edge maximum (Fig. 1, feature c) and one to two higher energy peaks (Fig. 1 feature c) are clearly visible in all spectra. These peaks are due to multiple scattering (MS) resonances of the photo-electron which depends on the local geometric structure. Both features b and c of Fig. 1 indicate a strong variation of the local atomic arrangement of Cu, paving the way for the analysis of the EXAFS portion of the XAS spectrum.

Table 1

Results of the analysis of the 1s-4p electronic transition of $[Cu(PTA)_4]BF_4$ obtained by XANES and EXAFS measurements.

Sample	Intensity (a.u.)	Center (eV)	Peak area (x100)	CN 1[a]
17 mM	0.39	8981.8	36(1)	4.0(3)
1.7 mM	0.41	8981.4	39.1(4)	3.2(3)
680 µM	0.46	8981.4	29.32(2)	2.8(4)
170 µM	0.44	8981.2	29.64(4)	2.9(4)
68 µM	0.47	8981.5	26.6(3)	2.4(5)

[a] CN 1 is defined here as the average number of bound PTA obtained by EXAFS analysis, see also Table 2.

Fig. 1B displays the comparison of the experimental Fourier Transform (FT) curves obtained by the corresponding EXAFS signals. The main peak is associated to the Cu-P first shell. The dramatic decrease in magnitude can be explained by the loss of a phosphine PTA ligand upon dilution. This trend is more pronounced in the 170 µM-17 mM range, and agrees with the feature a behavior of the XANES in Fig. 1. Unlike, the traces of the last two spectra (68 and 170 µM) appear broader in the peak around 1.8 Å, therefore suggesting a wider distribution of the Cu first shell distances compared to the species predominant at higher complex concentrations.

3.2 XAS studies - EXAFS analysis and structural model

To gain a complete understanding of the local atomic arrangement of Cu(I) in the different concentrated aqueous solutions of $[Cu(PTA)_4]BF_4$, an EXAFS analysis has been performed. This is the most suitable approach which can lead to the number of phosphine ligands coordinating the metal site and also allows the verification of the Cu-P bond length distance and associated structural disorder.

To this end, by referring to the Scheme 1, and considering the high symmetry of the PTA ligand, the parameterization of the $[Cu(PTA)_4]BF_4$ structure is relatively easy, and only few important Multiple Scattering (MS) signals are relevant to explain the overall EXAFS spectrum. They have been calculated as indicated in the Experimental Section, using a simplified model (Fig. S17) based on the atomic coordinates observed in the solid state.[11,12] The following n-body terms have been then included in the fitting procedures: the two-atom contributions $\gamma^{(2)}$ Cu-P with degeneracy of four, the three-body contribution $\gamma^{(3)}$ Cu-P-C with degeneracy of twelve (four adamantane). It is noteworthy that the inclusion of the three-body term $\gamma^{(3)}$ allows monitoring the shells beyond the first one by using the same three-atom coordinates both for the two-atom and the three-atom contributions. As such, the three-body signal $\gamma^{(3)}$ Cu-P-C includes both $\gamma^{(2)}$ Cu-C and $\gamma^{(3)}$ Cu-P-C contributions.

At first, the EXAFS analysis of the $Cu[PTA]_4BF_4$ in the solid state have been performed, which structure has been already identified by X-ray crystallography.[11,12] This ensures the reliability of the proposed data analysis, indicating an agreement with literature data. Fig. 2 displays the EXAFS fitting approach of the solid sample, in terms of both EXAFS (panel a) and the corresponding Fourier Transform (panel b). Both panels, displaying the comparison of the theoretical and experimental signals, are characterized by a perfect match of the two curves, thus testifying the accuracy of the present approach and the goodness of the fitting procedures. The

single EXAFS contributions visible in panel (a) set the structural limit of the electron scattering probe in this application. Only two individual signals are important in the determining the total theoretical one, *i.e.* the one relative to the four Cu-P first shell interaction (the highly relevant) and the one relative to the Cu-P-C three body contribution. This in turn means that EXAFS is capable to probe mainly the first coordination shell around Cu(I). Certainly, additional information includes the C-P bond length and the Cu-P-C angle. Overall, the atomic fragment probed by EXAFS is the one depicted in Fig. S17. The magnification of the residual curve displayed at the bottom of Fig. 3 indicates a very small portion of signal not included in the fitting procedure which is related to contributions at higher frequency. Their inclusion would only have the effect of an increased number of floating variable for the fitting, making the procedure less reliable. Table 2 summarizes the structural results as obtained by this fitting procedure.

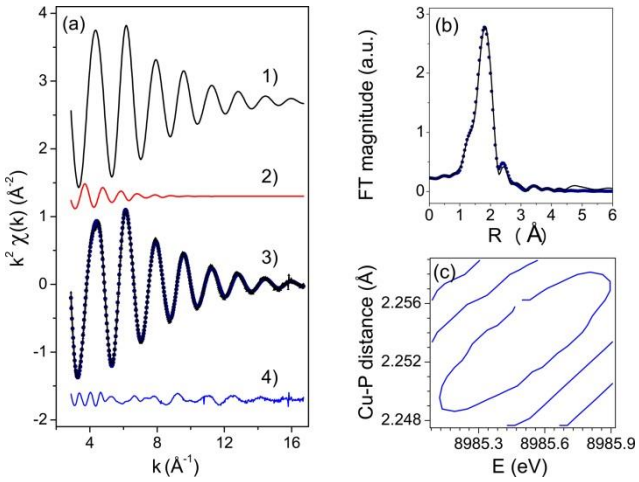

Fig. 2. a) Best fit of the Cu K-edge EXAFS signals for $[Cu(PTA)_4]BF_4$ solid sample. 1) EXAFS two-body $\gamma^{(2)}$ Cu-N contribution; 2) EXAFS two-body $\gamma^{(3)}$ Cu-N-C contribution; 3) experimental EXAFS spectrum (line) and calculated one (dotted); 4) Residual EXAFS signal; b) Fourier

Transform of the corresponding EXAFS signal; c) CONTOUR plot for the determination of the associated error to the Cu-P bond length.

Table 2

Structural parameters from EXAFS fitting results of spectra of $[Cu(PTA)_4]BF_4$ at different concentrations, and in the solid state. The estimated parameter errors are indicated in parentheses.

	$[Cu(PTA)_4]BF_4$ concentration					
	solid	17 mM	1.7 mM	680 µM	170 µM	68 µM
Cu-P / Å	2.253(5)[a]	2.258(5)	2.24(1)	2.23(1)	2.22(3)	2.27(3)
σ^2 Cu-P / Å^2	0.0058(5)	0.0042(8)	0.006(2)	0.0059(15)	0.015(3)	0.008(3)
Cu-O / Å	-	-	-	-	2.38(6)	2.32(2)
σ^2 Cu-O / Å^2	-	-	-	-	0.014	0.007(6)
θ^1 (Cu-P-C)/ deg	122(3)	123(2)	122(3)	122(3)	122(3)	n.d.
σ^2 θ^1 (Cu-P-C)/ deg^2	25(15)	46(20)	52(30)	12(10)	13(10)	n.d.
P-C / Å	1.87(3)[b]	1.87(3)	1.87(5)	1.88(5)	1.88(5)	n.d.
σ^2 P-C / Å^2	0.013(8)	0.03(1)	0.012	0.025	0.034	n.d.
CN 1 (Cu-P)	4.0	4.0(3)	3.2(3)	2.8(4)	2.9(4)	2.4(5)
CN 2 (Cu-O)	-	-	-	-	1.0(6)	1.2(7)
E_0 Cu	8985.5(6)	8984.9(5)	8983(1)	8982(1)	8979(2)	8984(4)
S_0^2 Cu	0.85(5)	0.76(5)	0.86(8)	0.76(8)	0.85(8)	0.76[c]
χ^2-like residual (x 10^{-6})	1.89	2.23	2.31	4.12	7.11	14.1

[a] Mean Cu-P distance in the solid state 2.284 Å, see ref. [11]. [b] Mean P-C distance in the solid state 1.852 Å, see ref. [11]. [c] Fixed value during refinement process.

The Cu-P bond length of 2.253(5) Å is found to be in complete agreement to the one obtained by the XRD,[9] and so the Cu-P-C bond angle of 122(3) degrees. Errors in the parameters have been obtained by CONTOUR plot,[40] as depicted in Fig. 3 c for the highly correlated and relevant Cu-P distance and E_0 variables (see below for details).

The EXAFS analyses of solutions of $[Cu(PTA)_4]BF_4$ were conducted using the same model and parameters adapted for the solid sample. Fig. S18 displays the best fit of the k^2-weighted EXAFS signals of 17 mM, 1.7 mM, 680 μM, and 170 μM solution of $[Cu(PTA)_4]BF_4$. Besides the usual higher noise of the experimental data at lower concentration, the theoretical curves match well within the experimental ones in all cases. The sinusoidal curves of the Fig. S18 appear rather similar for all investigated solutions apart of the intensity of the oscillations. This is consistent with the experimental FT curve behavior depicted in Fig. 1b and may be due to a loss of PTA ligand at the Cu core in dilute systems.

Figs. 3 and 4 reports the details of the EXAFS analysis in terms of single contribution to the total theoretical signal, for a selection of solutions. A list of the structural and non-structural parameters obtained from the best fits is presented in Table 2, together with their associated errors. As seen in Fig. 3 the same Multiple Scattering (MS) signals used for the solid sample are necessary to model the local structure of Cu in 17 mM, 1.7 mM, 680 μM solutions, and once again the two-body $\gamma^{(2)}$ Cu-P is contributing largely to the overall signal. This permits to check the number of PTA ligands coordinated to the Cu core (hereafter indicated as CN 1) with high relevance. This number is 4.0(3) at 17 mM, and progressively decreases to 3.2(3) and 2.8(4) at 1.7 mM and 680 μM respectively.

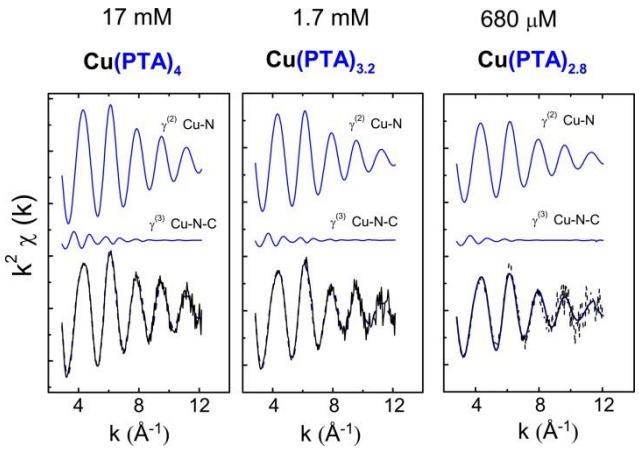

Fig. 3. Details of the EXAFS analysis of $[Cu(PTA)_4]BF_4$ at 17 mM, 1.7 mM and 680 μM solution. The figure shows the individual EXAFS contributions in terms of two-body and three-body signals to the total theoretical signal. The comparison of the total theoretical signal (lines) with the experimental one (dots) is also reported.

Unlike this set of solutions, the fit of the more diluted solutions (170 and 68 μM) requires a modification of the structural model, as indicated in Fig. 4. Out of several number *n* of P ligands, an additional O is required. The utilized individual EXAFS contributions are reported, as well as the comparison of the total theoretical signal to the experimental one. Due to higher noise of this experiment, the fitting procedure has been computed on k-weighted. Only the signals related to the first shell, the Cu-P and the Cu-O, are relevant. Following the best fit EXAFS outcome reported in Table 2, the coordination environment for Cu at 68 μM is described by a Cu core of 2.4 phosphine PTA ligands plus an oxygen of a coordinated water molecule. This is a quite remarkable result, considering the difficulty of recording a statistically significant EXAFS data at extremely low concentration.

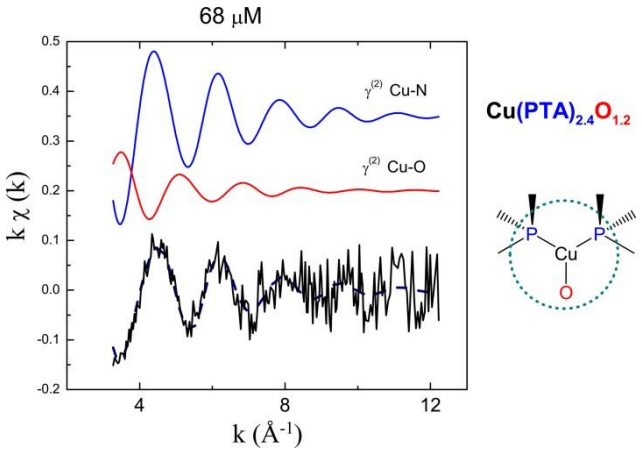

Fig. 4. EXAFS analysis of $[Cu(PTA)_4]BF_4$ at 68 μM solution. The figure shows the individual EXAFS contributions in terms of two-body (blue) and three-body (red) signals to the total theoretical signal. The total theoretical signal is reported (dashed blue) along with the experimental one (black). A scheme of the proposed predominant coordination sphere of Cu(I) at 68 μM is reported on the right side.

Data of Table 2 deserve a special attention because all the structural parameters of the Cu-P interaction are playing a key role. They are the Cu-P bond length, the corresponding bond variance γ^2 Cu-P and the number of PTA ligands (CN 1). As anticipated, the $[Cu(PTA)_4]^+$ species undergoes partial dissociation of PTA ligands upon dilution: actually, CN 1 diminishes from 4.0(3) to 2.4(5) upon 250-fold dilution of the initial 17 mM solution. The Cu-P first shell distance remains relatively the same along the series apart a lengthening observed for the 68 μM solution. The Cu-P bond variance values are in the 0.004 - 0.008 $Å^2$ range, with the exception of that for the 170 μM solution. These bond distance values are consistent to those found by EXAFS for similar phosphine complexes.[16,41] However, a higher steric hindrance holds here and this may be the cause of the difference. Concerning the Cu-O interaction, its value of 2.32

and 2.38 Å for the more diluted solutions is found to be consistent to coordinating water molecule.[42] An eye catching of the Cu-P ligation structural parameters and relative errors is presented in Fig. 5. Conclusions from this plot are: i) the Cu-P bond length decreasing upon dilution takes place with statistical significance; ii) the 68 µM solution is not following this rule (Cu-P lengthens), suggesting a different structural model; iii) the bond variance is almost the same for 17 mM, 1.7 mM, 680 µM solutions.

An additional aspect arising from the analysis of Table 2 is that the CN 1 calculated from data at 170 µM solution does not fit the overall decreasing trend observed upon dilution of the $[Cu(PTA)_4]BF_4$. This information, coupled with the observed high σ^2 Cu-P value (at least twice that observed for other solutions) suggests that profund changes in the structure of the species in solution likely pivot around this concentration, and that the average structural model may remain somewhat questionable for this sample. Nevertheless, we believe that overall these results show that a Cu-P coordination number decreasing upon dilution (CN 1 of Table 2) is observed. In fact, as coordination numbers and bond variance are typically very correlated parameters in EXAFS, a suspicious behavior could be anticipated in case of an inverse variation of the two parameters, which is definitively not our case.

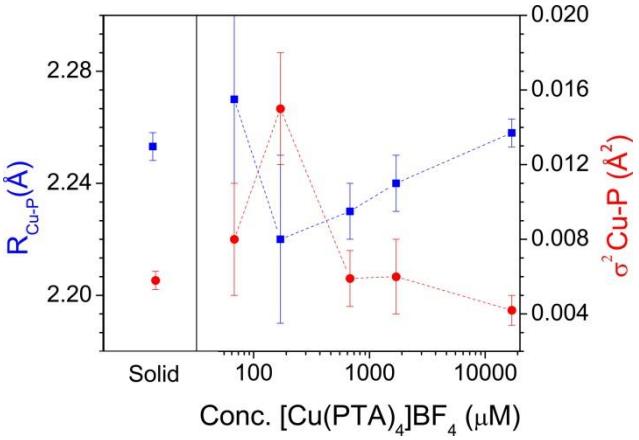

Fig. 5. Cu-P first shell bond distance and relative bond variance, for the entire series of spectra as obtained by the EXAFS fitting analysis.

The error in the parameters of Table 2 have been determined by using the contour plots (Fig. S2). These plots were selected among the parameters having strong correlation to reflect the highest error. The inner elliptical contour corresponds to the 95% confidence level. The plot at the bottom (right panel) is particularly relevant, as it is related to the Cu-P and Cu-O coordination number of the solution at 68 μM. Also, the 95% confidence level region can be identified in the plot and corresponds to the 2.4(5) *vs*. 1.2(7) Å for Cu-P and Cu-O interactions, respectively.

3.3 Potentiometric studies of the protonation equilibria of $[Cu(PTA)_4]^+$

We carried out the study of the protonation equilibria of $[Cu(PTA)_4]^+$ in aqueous solution (I = 0.1 M KCl) and, for the sake of completeness, of PTA. As it regards the ligand, PTA behaves as a monoprotic base in aqueous solution. Its protonated form $H(PTA)^+$ presents a pK_a = 5.70(1) likely associated to the deprotonation of a rigid, tertiary NH^+ function. This value is fully consistent with that previously reported in the literature.[19,39]

The potentiometric data for the titration of $[Cu(PTA)_4]^+$ were collected on samples at *ca*. 2 mM concentration of the complex, and showed that $[Cu(PTA)_4]^+$ complex is a tetraprotic base. The most protonated $[Cu(PTA)_4H_4]^{5+}$ form presents pK_{a1} = 3.63(2), pK_{a2}= 4.00(3), pK_{a3}= 4.28(3) and pK_{a4}= 5.11(4). These values are in agreement with the reported protonation constants of coordinated PTA in different $[Cu(PTA)_n]^+$ complexes in 1 M NaCl aqueous solution.[19] Also,

they are only *ca*. 1 log unit higher than those reported for PTA complexes with Re(II) and Ru(II).[43,44]

Although XAS data suggest that *ca*. 0.8 eq. of PTA are dissociated for a 2 mM complex concentration (Table 2, see 1.7 mM concentration), the best fitting of the potentiometric curve was obtained using a model where $[Cu(PTA)_4]^+$ is considered undissociated in solution. Conversely, no satisfactorily fitting of the experimental data could be obtained in the hypothesis that $[Cu(PTA)_3]^+$ is present in solution as the major species, along with an equimolar amount of free PTA (see Supporting Information, Fig. S15). Although this observation may sound contradictory, partial PTA dissociation is actually reflected into the stepwise differences between the pK_a values. While the ΔpK_a values are *ca*. 0.3 log units for the first three dissociation steps, that between pK_{a3} and pK_{a4} is *ca*. 0.9 log units, with pK_{a4} = 5.11. In the consideration that each single PTA binds only one proton,[39,43] this datum is in agreement with the partial dissociation of PTA that, as a free ligand, presents a higher pK_a (5.70). The presence of this dissociation process prevents the very precise determination of the pK_a's of $[Cu(PTA)_4]^+$; nevertheless it is clear that $[Cu(PTA)_4]^+$ is completely not protonated at physiological pH (7.4).

3.4 Spectrophotometric study of the formation equilibria of Cu(I)/PTA complexes

The study of the stability of the species formed by Cu(I) and PTA related with the determination of the equilibrium constants of the Cu(I) + nPTA = $[Cu(PTA))_n]^+$ formation equilibria. The strategy we used was to carry out competition spectrophotometric titrations of solutions of $[Cu(PTA)_4]BF_4$ with the metallochromic indicators bicinchoninate (BCA^{2-}) and bathocuproinedisulfonate (i-BCS^{2-}, Scheme 2). This approach is analogous to that we used

recently for the study of the stability of the $[Cu(thp)_4]^+$ complexes.[18,19] The use of BCA^{2-} and i-BCS^{2-} is convenient since these ligands form very stable Cu(I) colored complexes, resistant to air oxidation, with absorption bands centered at λ_{max} = 560 and 482 nm, respectively.[30,31] Noteworthy, these dyes have been previously used to elucidate aspects related to the thermodynamic-driven trafficking of Cu(I) by proteins,[30,33,45–47] and to prepare antiproliferative Cu(I) mixed-ligand complexes with tertiary phosphines which exhibited antiproliferative activity against tumor cell lines.[48]

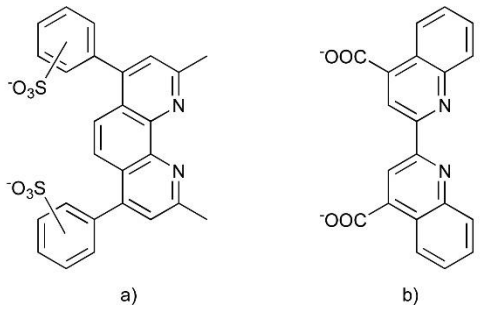

Scheme 2. a) i-BCS^{2-}; b) BCA^{2-}.

The samples used for spectrophotometric titrations contained *ca*. 74 μM $[Cu(PTA)_4]^+$, which is close to the lowest concentration used for XAS experiments (68 μM). The use of low concentration of analytes was required by the high molar absorbance of the Cu(I)-indicator adducts, and by the relative high affinities of the latter dyes for the copper(I) ion. At these analytical concentrations 2.4 phosphine ligands are coordinated to copper(I) together with a variable number of water molecules, as showed by XAS. This in turn implies that the $[Cu(PTA)_2]^+$ and $[Cu(PTA)_3]^+$ species are present at the equilibrium in a *ca*. 3:2 ratio (see Supporting Information). Under these circumstances neither one of the two $[Cu(PTA)_2]^+$ or

$[Cu(PTA)_3]^+$ species is predominant, and both should be taken into account in the treatment of spectroscopic data (see below). However, the study of the speciation of the Cu(I)/PTA system required the use of both BCA^{2-} and i-BCS^{2-} indicators (the reasons are discussed here below along with experimental observations). These dyes are bidentate ligands which form copper(I):ligand 1:1 and 1:2 complexes, where the latter is tetrahedral. The formation constants in aqueous solution of $[Cu(BCA)_2]^{3-}$ and $[Cu(i\text{-}BCS)_2]^{3-}$ complexes are known,[30–33,45–47,49,50] along with the crystal structure of the former anionic complex in a protonated form.[51]

While there is a general consensus on a formation log β = 19.8 for $[Cu(i\text{-}BCS)_2]^{3-}$,[30–33] a wider interval of log β values for $[Cu(BCA)_2]^{3-}$ is reported in the literature (11.4-17.2).[33,45–47,49,50] This discrepancy prompted us in re-determining the formation constant of the latter species. Also, we have re-determined the molar spectra and the formation constants of all copper(I) complexes with BCA^{2-} and i-BCS^{2-}, with the exception of that of $[Cu(i\text{-}BCS)_2]^{3-}$ (log β = 19.8) used as the only fixed parameter.[30–33]

The details of the re-determination of the spectral parameters and of the log β values of the complexes formed by Cu(I) with BCA^{2-} and i-BCS^{2-} are reported in the Supporting Information, and the final results summarized in Table 3. Here we briefly describe the strategy that we have used for their determination. We first performed an UV-Vis titration of a solution of $[Cu(CH_3CN)_4]BF_4$ with i-BCS^{2-} (see Supporting Information, Figs. S3-S5), and we treated the spectra dataset using log β = 19.8 for $[Cu(i\text{-}BCS)_2]^{3-}$.[30–33] This titration allowed us to determine the molar spectra of $[Cu(i\text{-}BCS)_2]^{3-}$ and of $[Cu(i\text{-}BCS)]^-$, along with the log β of the latter species (see Table 3). The second step was to determine the log β of the Cu(I) / BCA^{2-} complexes. Since the log β $[Cu(BCA)_2]^{3-}$ was expected higher than 12, we realized we could not

be able to determine it by direct titration of $[Cu(CH_3CN)_4]BF_4$ with BCA^{2-}. We decided therefore to determine the log β $[Cu(BCA)_2]^{3-}$ by competitive UV-Vis titration of a Cu(I)/BCA^{2-} 1:2 solution with i-BCS^{2-} (see Supporting Information, Figs. S6-S8). The treatment of this dataset allowed us to observe the formation of a mixed $[Cu(BCA)(BCS)]^{3-}$ species, of which the log β and molar absorbance were determined along with those of $[Cu(BCA)_2]^{3-}$ (see Table 3). With the log β of $[Cu(BCA)_2]^{3-}$ on our hands (16.7(1), Table 3), we have recorded and treated the spectral dataset of a UV-Vis titration of a solution of $[Cu(CH_3CN)_4]BF_4$ with BCA^{2-}(Supporting Information, Figs. S9-S11). This experiment allowed us to determine the log β $[Cu(BCA)]^-$ and accurate molar absorbance spectra of $[Cu(BCA)_2]^{3-}$ and $[Cu(BCA)]^-$. The spectral (λ_{max}, ε) and thermodynamic (log β) parameters of the various Cu(I) complexes of BCA^{2-} and i-BCS^{2-} are reported in Table 3, and they are overall consistent with those reported previously in the literature.[20,30,32]

Table 3

Log β values, wavelength of the absorption maxima in the visible range (λ_{max}), and related molar absorbances (ε) for the complex species of copper(I) with the metallochromic indicators BCA^{2-} and i-BCS^{2-}.

Species	log β	λ_{max} (nm) / ε (M^{-1} cm^{-1})
$[Cu(BCA)]^-$	8.73(2)	560 / 2300
$[Cu(BCA)_2]^{3-}$	16.7(1)	559 / 7840
$[Cu(i\text{-}BCS)]^-$	10.0(1)	482 / 13350
$[Cu(i\text{-}BCS)_2]^{3-}$	19.8[30–33]	482 / 3830
$[Cu(BCA)(i\text{-}BCS)]^{3-}$	18.6(1)	540 / 8260

$[Cu(PTA)_2(BCA)]^-$	23.2(2)	405 / 4270
$[Cu(PTA)_2(i\text{-}BCS)]^-$	24.3(1)	374 / 5500

We initially attempted the determination of the stability constant of the $[Cu(PTA)_n]^+$ species by UV-vis titration of an aqueous solution of $[Cu(PTA)_4]BF_4$ with the metallochromic indicator bicinchoninate (BCA^{2-}). Through this experiment we previewed we could see the ligand substitution and formation of the $[Cu(PTA)_2(BCA)]^-$ species first, followed by $[Cu(BCA)_2]^{3-}$. The occurrence of these processed would have allowed us to determine the formation constant of the $[Cu(PTA)_n]^+$ species by one single UV-vis competition titration experiment as we reported recently for $[Cu(thp)_n]^+$.[20]

The UV-Vis titration of a 74 μM aqueous solution of $[Cu(PTA)_4]BF_4$ (100 mM HEPES, pH 7.4) with BCA^{2-} resulted into an unexpected behavior. The spectral dataset is reported in Fig. 6. One single band appeared in the 375-700 nm range (λ_{max} *ca*. 405 nm), which reached its maximum in correspondence of the addition of 1 eq. of BCA^{2-} with respect of Cu(I) (Fig. 7). Unexpectedly, in the presence of an excess of BCA^{2-} (2.3 eq. vs. Cu(I)), no bands at 560 nm associated to the formation of the $[Cu(BCA)_2]^{3-}$ appeared. Overall this spectral dataset suggests that by titration of a 74 μM solution of $[Cu(PTA)_4]^+$ with BCA^{2-}, a mixed $[Cu(PTA)_2(BCA)]^-$ is formed, but also that successive addition of extra 1.3 eq. of BCA^{2-} does not result in the displacement of the last two coordinated PTA ligands to give the $[Cu(BCA)_2]^{3-}$ species. It is worth noting that we have isolated this $[Cu(PTA)_2(BCA)]^-$ complex and characterized it in the solid state by X-ray diffraction, in the form of a mixed-valence $\{Cu(II)[Cu(I)(BCA)(PTA)_2]_2\}$ species. Although we tried several conditions including the absence of oxygen, we isolated the Cu(I) mixed-ligands species only by slow evaporation of the mother liquors from the synthesis of

[Cu(BCA)Na(PTA)$_2$]·NaBF$_4$.[48] Its structural characterization is reported in the Supporting Information.

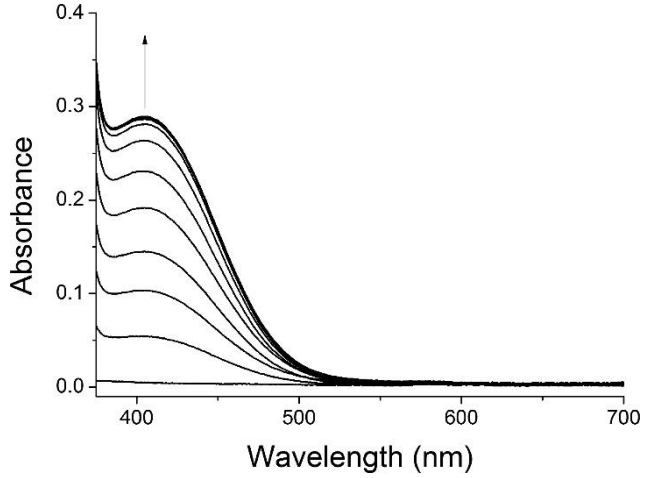

Fig. 6 Spectra for the titration of a solution of [Cu(PTA)$_4$]BF$_4$ (C_{Cu} = 74 μM) with BCA^{2-} in aqueous HEPES buffer (100 mM, pH 7.4; Cu(i):BCA^{2-} = 1:0-2.3).

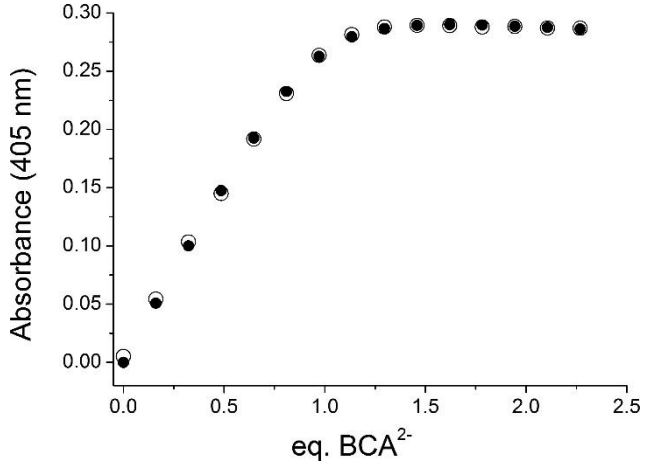

Fig. 7. Experimental (○) and calculated (●) absorbance values at 405 nm for the titration of a solution of [Cu(PTA)$_4$]BF$_4$ (C_{Cu} = 74 μM) with BCA^{2-} in aqueous HEPES buffer (100 mM, pH 7.4).

Since XAS data suggested that in diluted samples $[Cu(PTA)_2]^+$ and $[Cu(PTA)_3]^+$ are the most abundant species (see above), the relevant equilibria in this titration are:

$$[Cu(PTA)_2]^+ + BCA^{2-} = [Cu(PTA)_2(BCA)]^- \quad (1)$$

$$[Cu(PTA)_3]^+ + BCA^{2-} = [Cu(PTA)_2(BCA)]^- + PTA \quad (2)$$

Which are described by two constants indicated here as $K^{P2}_{CuP2BCA}$ and $K^{P3}_{CuP2BCA}$, respectively (P = PTA):

$$K^{P2}_{CuP2BCA} = \frac{[Cu(PTA)_2(BCA)]}{[Cu(PTA)_2][BCA]} \quad (3)$$

$$K^{P3}_{CuP2BCA} = \frac{[Cu(PTA)_2(BCA)][PTA]}{[Cu(PTA)_3][BCA]} \quad (4)$$

Fig. 7 shows that the absorbance change at the titration end-point (1 eq. BCA^{2-}) is smooth. This indicates that if the log β of the $[Cu(PTA)_2(BCA)]^-$ is made available along with $K^{P2}_{CuP2BCA}$ and $K^{P3}_{CuP2BCA}$, the log β values of the $[Cu(PTA)_2]^+$ and $[Cu(PTA)_3]^+$ can be calculated as:

$$\log \beta_{[Cu(PTA)2]} = \log \beta_{Cu(PTA)2(BCA)} - \log K^{P2}_{CuP2BCA} \quad (5)$$

$$\log \beta_{[Cu(PTA)3]} = \log \beta_{Cu(PTA)2(BCA)} - \log K^{P3}_{CuP2BCA}. \quad (6)$$

The dataset for the titration of $[Cu(PTA)_4]BF_4$ with BCA^{2-} reported in Fig. 6 was used to calculate the equilibrium constant of equilibrium (1) ($K^{P2}_{CuP2BCA}$, eqn. 3), taking into account that the concentration of the species $[\{Cu(PTA)_2(BCA)\}^-]$ relates with the absorbance through the Lambert Beer equation:

$$A^{405\ nm} = \varepsilon^{405\ nm} \cdot [\{Cu(PTA)_2(BCA)\}^-] \quad (7)$$

It can be demonstrated (see calculations in the Supporting Information) that the concentration of [{$Cu(PTA)_2(BCA)\}^-$] can be expressed as:

$$[Cu(PTA)_2BCA] = \frac{\left[\frac{3}{5}K^{P2}_{CuP2BCA}(T_{Cu}+T_{BCA})+1\right]}{\frac{6}{5}K^{P2}_{CuP2BCA}} + - \frac{\sqrt{\left[\frac{3}{5}K^{P2}_{CuP2BCA}(T_{Cu}+T_{BCA})+1\right]^2 - \frac{36}{25}\left(K^{P2}_{CuP2BCA}\right)^2 T_{Cu}T_{BCA}}}{\frac{6}{5}K^{P2}_{CuP2BCA}} \quad (8)$$

Equation (8) was introduced into equation (7) and the obtained equation was used to treat through least-square procedure the data in Fig. 6 (in the 390-410 nm range) to calculate the log $K^{P2}_{CuP2BCA}$ parameter which resulted 6.24(4).

In order to calculate log $\beta_{[Cu(PTA)2]}$ using eq. (5), the value of the log β of the mixed $[Cu(PTA)_2(BCA)]^-$ complex (log $\beta_{Cu(PTA)2(BCA)}$) was required. This parameter has been determined by means of a competition titration with i-BCS^{2-} of a solution $[Cu(PTA)_4]^+$ / BCA^{2-} in 1:1.1 ratio, where the $[Cu(PTA)_2(BCA)]^-$ species dominates. The spectra dataset of these experiments is reported in Fig. 8. For the addition of 1 eq. of i-BCS^{2-} a first family of spectra was observed, associated with the appearance of an isosbestic point at 396 nm and a decrease of absorbance at 405 nm. The second family of spectra was observed after the addition of 1 eq. of i-BCS^{2-}, with an increase of absorbance at 480 nm. These spectral trends suggest that $[Cu(PTA)_2(BCA)]^-$ first converts into $[Cu(PTA)_2(i\text{-}BCS)]^-$, and then into $[Cu(i\text{-}BCS)_2]^{3-}$ in the excess of i-BCS^{2-}. A detailed analysis of this experiment is reported in Supporting Information, and the quantitative data treatment is in agreement with this reaction model.

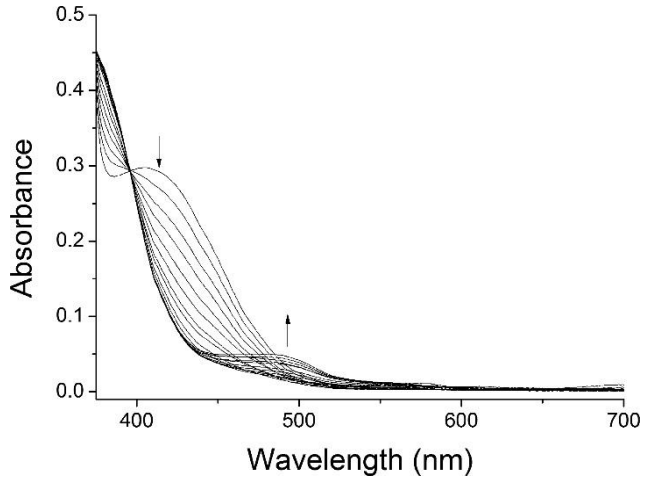

Fig. 8. Spectra for the titration of a solution of $[Cu(PTA)_4]BF_4$ and BCA^{2-} 1:1.1 (C_{Cu} = 74 μM) with i-BCS^{2-} in aqueous HEPES buffer (100 mM, pH 7.4). Cu(I):i-BCS^{2-} = 1:0-2.6).

In the titration with i-BCS^{2-} of a solution $[Cu(PTA)_4]^+$ and BCA^{2-} two successive equilibria come into play, namely:

$$[Cu(PTA)_2(BCA)]^- + \text{i-}BCS^{2-} = [Cu(PTA)_2(\text{i-}BCS)]^- + BCA^{2-} \quad (9)$$

$$[Cu(PTA)_2(\text{i-}BCS)]^- + \text{i-}BCS^{2-} = [Cu(\text{i-}BCS)_2]^{3-} + 2\ PTA \quad (10)$$

While equilibrium (9) is relevant for additions of i-BCS^{2-} up to 1 equivalent, successive addition of the latter ligand trigger the appearance of the second equilibrium (10). We have treated this spectral dataset though the software HyperQuad 2006 using log β = 19.8 for $[Cu(\text{i-}BCS)_2]^{3-}$, obtaining the simultaneous determination of the log β values of both $[Cu(PTA)_2(BCA)]^-$ and $[Cu(PTA)_2(\text{i-}BCS)]^-$ (23.2(2) and 24.3(1), respectively).

With the values of the two parameters log $\beta_{CuP2BCA}$ (23.2(2)) and log $K^{P2}_{CuP2BCA}$ (6.24(4)) in our hands, we could actually calculate log $\beta_{[Cu(PTA)2]}$ using eq. (5), which resulted 17.0(2). The log $\beta_{[Cu(PTA)3]}$ could be then calculated using the equation

$$\frac{\beta_{[CuP2]}}{\beta_{[CuP3]}} = \frac{[CuP_2]}{[Cu][PTA]^2}\frac{[Cu][PTA]^3}{[CuP_3]} = [PTA] \quad (11)$$

By recalling that $[CuP_2]/[CuP_3]$ =3/2 at 68 μM total copper concentration as suggested by XAS data, eq. (11) can be rearranged into

$$\beta_{[CuP3]} = \frac{2}{3}\frac{\beta_{[CuP2]}}{[PTA]} \quad (12)$$

The [PTA] can be calculated by mass balance equations for [Cu(I)] and [PTA], for a 68 μM $[Cu(PTA)_4]^+$ solution and in the hypothesis that $[Cu(PTA)_2]^+$ or $[Cu(PTA)_3]^+$ species are the two relevant species in ratio 3:2, resulting into [PTA] = 109 μM. The calculated value for log $\beta_{[Cu(PTA)3]}$ results 20.8. The estimation of the standard deviation can be done by considering that the calculated average number of coordinated phosphines is 2.4(5) (Table 2). Since for this parameter the relative error is 20%, we can estimate a similar precision for $\beta_{[Cu(PTA)3]}$, leading to log β = 20.8(2) as the best value for this parameter.

Two parameters are left undetermined at this stage, namely the log β values of the $[Cu(PTA)]^+$ and that of the $[Cu(PTA)_4]^+$ species. Actually, speciation simulations carried out through Hyss 2009 using log β values determined here for $[Cu(PTA)_2]^+$ and $[Cu(PTA)_3]^+$, and 8.9 estimated for $[Cu(PTA)]^+$,[19] showed that the concentration of the latter species is negligible for a total concentration of $[Cu(PTA)_4]BF_4$ of 68 μM. For this reason, the log β of the $[Cu(PTA)]^+$ is not accessible with our data and therefore it is left undetermined in our speciation model.

In order to obtain a reliable estimation of the log β value of the $[Cu(PTA)_4]^+$ species we have taken into account the XAS data. In particular, the number of coordinated phosphines at different

$[Cu(PTA)_4]BF_4$ concentrations were used as restraints for the estimation of the thermodynamic parameter (see Table 2). We have considered an initial value of log β for $[Cu(PTA)_4]^+$ of 24, along with the determined values of the log β of the $[Cu(PTA)_2]^+$ and $[Cu(PTA)_3]^+$ species. The log β for $[Cu(PTA)_4]^+$ of has been iteratively refined it by calculation of the average number of phosphine ligands at 17 mM, 1.7 mM, 680 μM and 68 μM total $[Cu(PTA)_4]BF_4$ concentration (CN 1 = $\chi_{Cu(PTA)2} \cdot 2 + \chi_{Cu(PTA)3} \cdot 3$). At each concentration, the molar fractions χ were calculated using the Hyss 2009 software. The CN 1 value at 170 μM was excluded since this value seems affected by a bias related to uncentainty in the structural model used for its determination (see above). Also, the species $[Cu(PTA)]^+$ was considered present at a negligible concentrations (see above). By changing iteratively the log β value of $[Cu(PTA)_4]^+$ we have refined its value by minimizing the sum of least square residuals between the calculated CN 1 and their experimental values (Table 2). The refined log β value resulted 23.4(2), and the calculated CN 1 were 2.4, 3.0, 3.2 and 3.7 for increasing $[Cu(PTA)_4]BF_4$ concentrations, which compare well with the values reported in Table 2.

The determined formation constants (log β values) of the $[Cu(PTA)_n]^+$ species are reported in Table 4, and a representative distribution diagram is reported in Fig. 9. Overall, our thermodynamic studies in 100 mM aqueous HEPES (pH 7.4) show that the log β values estimated for a chloride-free medium are, as expected, higher than the corresponding determined in 1M NaCl aqueous solution. Also, data in Table 4 show that the log β values determined experimentally here in the absence of chloride are intermediate between those determined in the presence of chloride ions, and those extrapolated for a medium where no Cl^- are present. $[Cu(PTA)_2]^+$ species is an exception, and its log β is one log unit higher than that estimated previously.[19] Interestingly, the remarkable stability of the $[Cu(PTA)_2]^+$ species is not

surprising, as this ion has been found as the major species in mass spectrometric studies on diluted $[Cu(PTA)_4]BF_4$ solutions.[18] Therefore, our speciation model determined by combining UV-Vis titration and XAS data is in good agreement with previous experimental observations.[18]

Table 4

Log β values of the $[Cu(PTA)_n]^+$ species in different aqueous media. Standard deviations are reported in parenthesis.

Species	Log β 1 M NaCl [a]	Log β no Cl^- [a]	Log β 100 mM HEPES
$[Cu(PTA)]^+$	6.3(2)	8.9(3)	n.d.
$[Cu(PTA)_2]^+$	12.1(1)	15.9(12)	17.0(2)
$[Cu(PTA)_3]^+$	17.7(2)	22.7(1)	20.8(2)
$[Cu(PTA)_4]^+$	21.4(2)	26.4(1)	23.4(2)

[a] See ref. [19]

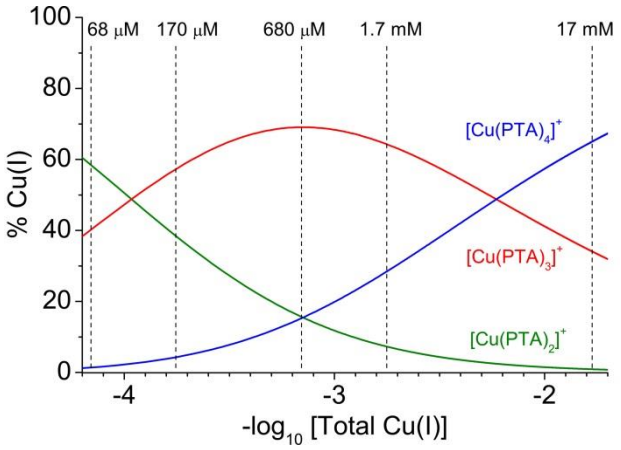

Fig. 9. Representative distribution diagram of $[Cu(PTA)_4]^+$ at different total copper(I) concentrations between 68 μM and 17 mM.

Importantly, in this study we have obtained the formation constants of Cu(I) (P_2,N_2) mixed complexes, that resulted remarkably stable in solution (Table 3). This is demonstrated, for instance, by the data reported in Fig. 8 where an excess of BCA^{2-} added to $[Cu(PTA)_2(BCA)]^-$ (up to BCA^{2-}:Cu(I) = 2.4) is not sufficient to observe the formation of $[Cu(BCA)_2]^{3-}$. We found this behavior extremely interesting, since it might indicate a great affinity of the $[Cu(PTA)_2]^+$ fragment for nitrogen donor atoms. Although we are aware of the difference between histidine nitrogen atoms and aromatic bidentate moieties, we believe that this behavior may indicate that the $[Cu(PTA)_2]^+$ species can be able to bind to the imidazole group of histidine leading us to put forward few considerations.

The first consideration relates with the observation that the mechanism of function of some Cu(I)/phosphine complexes may involve their interaction with the copper binding sites of human copper transporter (hCTR).[20] Actually, the extracellular domain of hCTR presents histidine residues.[52,53] We therefore put forward the hypothesis that PTA as coligands may favor the interaction of copper(I) with those binding sites and favor the internalization of copper. In this way, the favorable formation of a mixed (N^{im}_n, P_2) adduct may be at the origin of a hCRT-dependent cytotoxicity of this class of compounds. In this respect, the possibility of the $[Cu(PTA)_n]^+$ fragments to coordinate chloride ions (as discussed in ref. [19]) may be important for their cytotoxicity. Actually, it is likely that the presence of chlorides and coligand prevents

the irreversible binding of the Cu/PTA fragments to donor groups such as amino acids residues until the final biomolecular target (*e.g.* hCTR) is reached.

The second consideration relates with the use of PTA as a competing ligand of β-amyloid (Aβ) in the complexation of Cu(I), in view of its possible use in copper chelation therapy for the treatment of neurodegenerative diseases such as Alzheimer disease.[54,55] Fig. 10 reports a representative distribution diagram of the competition between Aβ and PTA in presence of Cu(I), at the concentrations reported in the literature for this experiment.[54] To draw this diagram the affinity constant of $A\beta_{1\text{-}16}$ for Cu(I) has been used ($7.5x10^6$ M^{-1}, HEPES 100 mM, pH 7.4).[33] The curves in the distribution diagram are consistent with the experimental data, in particular with the formation of $[Cu(PTA)_3]^+$ and $[Cu(PTA)_4]^+$ in the excess of PTA. Since the two species have a very similar spectrum in the EXAFS region (Fig. 1), small differences in the XAS spectra can be accounted by kinetic effects.

Although the Cu(I)/PTA 1:2 conditions were not explored in the experiment, it is interesting to see that the $[Cu(PTA)_2]^+$ species is predominant, although only for that metal:ligand ratio. However, if a similar speciation diagram is drawn for a 1000-fold diluted analytes (*i.e.* Cu(I)/Aβ at uM concentrations, see Supporting Information), the $[Cu(PTA)_2]^+$ is basically the only species present in solution even for a 6-fold excess of PTA. On one hand, this observation further confirms that this fragment has to be taken always into account when to interpret the reactivity of PTA with Cu(I) in diluted conditions, especially in terms of possible formation of ternary species. On the other hand, our results tell that for the Cu(I)/Aβ system it will be interesting in the future to explore the possibility that Cu(I) is involved in the formation of a unreactive, mixed (N^{im}_2, P_2) coordination, rather than completely extracted from its adduct with the amyloid

peptide. This behavior may result predominant given the low local concentrations of these species that should exist in biological environment.

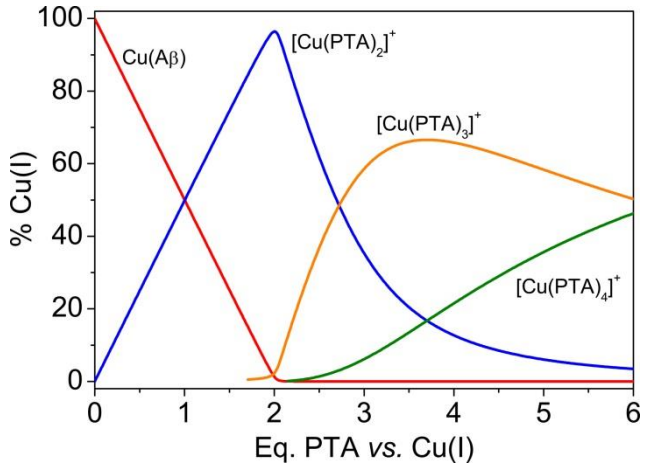

Fig. 10. Representative distribution diagram for the addition of PTA to a Cu(I) / β-amyloid (Aβ) system (Cu: Aβ = 1:1.1, $C_{Cu(I)}$ = 0.9 mM). Charges omitted for the Cu(I)/Aβ adduct.

4. Conclusions

In this paper we have shed light into the structure and the stability of the $[Cu(PTA)_4]^+$ species in aqueous solution and at different concentrations. In particular, we have studied samples down to 68 μM, which is a concentration that may be relevant for the study of the biological role of this complex. Although these concentrations were straightforwardly accessed by spectrophotometry using metallochromic indicators, the same was not predicted for XAS data. Perhaps unexpectedly, the latter technique has provided with extraordinary pieces of information on the first coordination sphere of Cu(I) at the various concentrations that in turn allowed the determination of the formation constants of the $[Cu(PTA)_n]^+$ species (n=2-4) in aqueous solution.

Our experimental formation constants are in very good agreement with those reported in the literature for pure aqueous conditions obtained by extrapolation of those determined in the presence of chloride ions.

Our speciation of both the Cu(I)/PTA and the Cu(I)/PTA/BCA^{2-}($i\text{-}BCS^{2-}$) systems allow to draw some interesting conclusions. The PTA ligand, although monodentate, forms with Cu(I) remarkably stable complexes and no free Cu(I) is present at significant level in 68 μM $[Cu(PTA)_4]BF_4$ samples. Of the observed $[Cu(PTA)_n]^+$ species (n=2-4) the $[Cu(PTA)_2]^+$ fragment results remarkably stable in solution. XAS data showed that Cu(I) in the latter species does not strictly possess a coordination number of 2, since water molecules are partially coordinated to the metal along with the two phosphines. Perhaps more important, the mixed $[Cu(PTA)_2(BCA/i\text{-}BCS)]^-$ species possess a remarkable thermodynamic stability which suggest that, although relatively stable, the $[Cu(PTA)_2]^+$ has the propensity to form adducts with N-donor ligands, possibly (N_2, P_2) coordinate. Finally, this last observation implies that the biological role of PTA, for instance in chelation therapy, may relate with the formation of stable and possibly less reactive mixed (N_2, P_2) complexes, rather than with a real competition with extraction of copper(I) from the bioligand. This hypothesis, where verified, may be of paramount importance in the future for devising new phosphine-based chelating agents for Cu(I) with applications in chelation therapy for neurodegenerative diseases.

Acknowledgments

The authors thank the Italian Interuniversity Consortium of Research in the Chemistry of Metal Ions in Biological Systems (CIRCMSB, Bari, Italy). The European Synchrotron Radiation Facility (ESRF) is acknowledged through the project # CH-3283 (principal investigator MG). M.D. wishes

to thank the EACEA for providing the 2-years scholarship through the "Advanced Spectroscopy in Chemistry" Erasmus Mundus Joint Master Degree European Programme. M.G. and M.T. equally contributed to this work.

Funding

This work was supported by the University of Bologna (RFO) and the University of Parma (FIL).

Appendix A. Supplementary material

Electronic Supplementary information (ESI) available: Crystallographic data for the structure reported in this paper have been deposited with the Cambridge Crystallographic Data Centre (CCDC) as supplementary publication number CCDC 1813009. Copies of the data can be obtained free of charge from the CCDC (12 Union Road, Cambridge CB2 1EZ, UK; Tel.: +44-1223-336408; Fax: +44-1223-336003; e-mail: deposit@ccdc.cam.ac.uk; web site: http://www.ccdc.cam.ac.uk). Supplementary data to this article (Plots of XAS data treatment, spectrophotometric titrations dataset, plot of the molar absorbances of the absorbing complex species, plot of the titration curve of $[Cu(PTA)_4]BF_4$, and representative distribution diagrams) can be found online at https://doi.org/10.1016/j.jinorgbio.XXXX.XX.XXX.

References

[1] A.D. Phillips, L. Gonsalvi, A. Romerosa, F. Vizza, M. Peruzzini, Coordination chemistry of 1,3,5-triaza-7-phosphaadamantane (PTA), Coord. Chem. Rev. 248 (2004) 955–993.

doi:10.1016/j.ccr.2004.03.010.

[2] J. Bravo, S. Bolaño, L. Gonsalvi, M. Peruzzini, Coordination chemistry of 1,3,5-triaza-7-phosphaadamantane (PTA) and derivatives. Part II. The quest for tailored ligands, complexes and related applications, Coord. Chem. Rev. 254 (2010) 555–607. doi:10.1016/j.ccr.2009.08.006.

[3] A. Guerriero, M. Peruzzini, L. Gonsalvi, Coordination chemistry of 1,3,5-triaza-7-phosphatricyclo[3.3.1.1]decane (PTA) and derivatives. Part III. Variations on a theme: Novel architectures, materials and applications., Coord. Chem. Rev. 355 (2018) 328–361. doi:10.1016/j.ccr.2017.09.024.

[4] D.N. Akbayeva, L. Gonsalvi, W. Oberhauser, M. Peruzzini, F. Vizza, P. Brüggeller, A. Romerosa, G. Sava, A. Bergamo, Synthesis, catalytic properties and biological activity of new water soluble ruthenium cyclopentadienyl PTA complexes $[(C_5R_5)RuCl(PTA)_2]$ (R = H, Me; PTA = 1,3,5-triaza-7-phosphaadamantane)., Chem. Commun. (2003) 264–5. http://www.ncbi.nlm.nih.gov/pubmed/12585422.

[5] S. Bolaño, L. Gonsalvi, F. Zanobini, F. Vizza, V. Bertolasi, A. Romerosa, M. Peruzzini, Water soluble ruthenium cyclopentadienyl and aminocyclopentadienyl PTA complexes as catalysts for selective hydrogenation of α,β-unsaturated substrates (PTA=1,3,5-triaza-7-phosphaadamantane), J. Mol. Catal. A Chem. 224 (2004) 61–70. doi:10.1016/j.molcata.2004.06.030.

[6] D.J. Darensbourg, F.A. Beckford, J.H. Reibenspies, Water-Soluble Organometallic Compounds. 8[1]. Synthesis, spectral properties, and crystal structures of 1,3,5-triaza-7-phosphaadamantane (pta) derivatives of metal carbonyl clusters: $Ru_3(CO)_9(PTA)_3$ and $Ir_4(CO)_7(PTA)_5$, J. Clust. Sci. 11 (2000) 95–107. doi:10.1023/A:1009060614412.

[7] R. Lee, S. Escrig, C. Maclachlan, G. Knott, A. Meibom, G. Sava, P. Dyson, The differential distribution of RAPTA-T in non-invasive and invasive breast cancer cells correlates with its anti-invasive and anti-metastatic effects, Int. J. Mol. Sci. 18 (2017) 1869. doi:10.3390/ijms18091869.

[8] B.S. Murray, M. V. Babak, C.G. Hartinger, P.J. Dyson, The development of RAPTA compounds for the treatment of tumors, Coord. Chem. Rev. 306 (2016) 86–114. doi:10.1016/j.ccr.2015.06.014.

[9] M. Porchia, F. Benetollo, F. Refosco, F. Tisato, C. Marzano, V. Gandin, Synthesis and structural characterization of copper(I) complexes bearing N-methyl-1,3,5-triaza-7-phosphaadamantane (mPTA), J. Inorg. Biochem. 103 (2009) 1644–1651. doi:10.1016/j.jinorgbio.2009.09.005.

[10] C. Santini, M. Pellei, G. Papini, B. Morresi, R. Galassi, S. Ricci, F. Tisato, M. Porchia, M.P. Rigobello, V. Gandin, C. Marzano, In vitro antitumour activity of water soluble Cu(I), Ag(I) and Au(I) complexes supported by hydrophilic alkyl phosphine ligands, J. Inorg. Biochem. 105 (2011) 232–240. doi:10.1016/j.jinorgbio.2010.10.016.

[11] A.M. Kirillov, P. Smoleński, M.F.C. Guedes da Silva, A.J.L. Pombeiro, The first copper complexes bearing the 1,3,5-triaza-7-phosphaadamantane (PTA) ligand, Eur. J. Inorg. Chem. 2007 (2007) 2686–2692. doi:10.1002/ejic.200601152.

[12] A.M. Kirillov, P. Smoleński, M.F.C. Guedes da Silva, M.N. Kopylovich, A.J.L. Pombeiro, Three-dimensional hydrogen-bonded supramolecular assembly in tetrakis(1,3,5-triaza-7-phosphaadamantane)copper(I) chloride hexahydrate, Acta Crystallogr. Sect. E Crystallogr. Commun. 64 (2008) m603–m604. doi:10.1107/S1600536808008179.

[13] S. Alidori, G. Gioia Lobbia, G. Papini, M. Pellei, M. Porchia, F. Refosco, F. Tisato, J.S. Lewis, C. Santini, Synthesis, in vitro and in vivo characterization of ^{64}Cu(I) complexes derived from hydrophilic tris(hydroxymethyl)phosphane and 1,3,5-triaza-7-phosphaadamantane ligands, J. Biol. Inorg. Chem. 13 (2008) 307–315. doi:10.1007/s00775-007-0322-y.

[14] P. Nowak-Sliwinska, J.R. van Beijnum, A. Casini, A.A. Nazarov, G. Wagnières, H. van den Bergh, P.J. Dyson, A.W. Griffioen, Organometallic ruthenium(ii) arene compounds with antiangiogenic activity, J. Med. Chem. 54 (2011) 3895–3902. doi:10.1021/jm2002074.

[15] A. Bergamo, Modulation of the metastatic progression of breast cancer with an

organometallic ruthenium compound, Int. J. Oncol. (1992). doi:10.3892/ijo_00000119.

[16] V. Gandin, A. Trenti, M. Porchia, F. Tisato, M. Giorgetti, I. Zanusso, L. Trevisi, C. Marzano, Homoleptic phosphino copper(I) complexes with in vitro and in vivo dual cytotoxic and anti-angiogenic activity, Metallomics. 7 (2015) 1497–1507. doi:10.1039/C5MT00163C.

[17] S. Tapanelli, A. Habluetzel, M. Pellei, L. Marchiò, A. Tombesi, A. Capparè, C. Santini, Novel metalloantimalarials: Transmission blocking effects of water soluble Cu(I), Ag(I) and Au(I) phosphane complexes on the murine malaria parasite Plasmodium berghei, J. Inorg. Biochem. 166 (2017) 1–4. doi:10.1016/j.jinorgbio.2016.10.004.

[18] F. Tisato, F. Refosco, M. Porchia, M. Tegoni, V. Gandin, C. Marzano, M. Pellei, G. Papini, L. Lucato, R. Seraglia, P. Traldi, The relationship between the electrospray ionization behaviour and biological activity of some phosphino Cu(I) complexes., Rapid Commun. Mass Spectrom. 24 (2010) 1610–6. doi:10.1002/rcm.4553.

[19] F. Endrizzi, P. Di Bernardo, P.L. Zanonato, F. Tisato, M. Porchia, A. Ahmed Isse, A. Melchior, M. Tolazzi, Cu(I) and Ag(I) complex formation with the hydrophilic phosphine 1,3,5-triaza-7-phosphadamantane in different ionic media. How to estimate the effect of a complexing medium, Dalton Trans. 46 (2017) 1455–1466. doi:10.1039/C6DT04221J.

[20] F. Tisato, C. Marzano, V. Peruzzo, M. Tegoni, M. Giorgetti, M. Damjanovic, A. Trapananti, A. Bagno, C. Santini, M. Pellei, M. Porchia, V. Gandin, Insights into the cytotoxic activity of the phosphane copper(I) complex $[Cu(thp)_4][PF_6]$, J. Inorg. Biochem. 165 (2016) 80–91. doi:10.1016/j.jinorgbio.2016.07.007.

[21] A. Hetherington, W. Levason, M.D. Spicer, Synthesis and copper-63 NMR studies of copper(I) stibine complexes, Polyhedron. 9 (1990) 1609–1612. doi:10.1016/S0277-5387(00)86580-8.

[22] F. d'Acapito, A. Trapananti, S. Torrengo, S. Mobilio, X-ray Absorption Spectroscopy: the Italian beamline GILDA of the ESRF, Not. Neutroni E Luce Di Sincrotrone. 19 (2014).

[23] B. Ravel, M. Newville, ATHENA , ARTEMIS , HEPHAESTUS : data analysis for X-ray

absorption spectroscopy using IFEFFIT, J. Synchrotron Radiat. 12 (2005) 537–541. doi:10.1107/S0909049505012719.

[24] A. Filipponi, A. Di Cicco, X-ray-absorption spectroscopy and n-body distribution functions in condensed matter. II. Data analysis and applications, Phys. Rev. B. 52 (1995) 15135–15149. doi:10.1103/PhysRevB.52.15135.

[25] M. Giorgetti, M. Berrettoni, A. Filipponi, P.J. Kulesza, R. Marassi, Evidence of four-body contributions in the EXAFS spectrum of $Na_2Co[Fe(CN)_6]$, Chem. Phys. Lett. 275 (1997) 108–112. doi:10.1016/S0009-2614(97)00724-0.

[26] L. Hedin, B.I. Lundqvist, Explicit local exchange-correlation potentials, J. Phys. C Solid State Phys. 4 (1971) 2064–2083. doi:10.1088/0022-3719/4/14/022.

[27] M.O. Krause, J.H. Oliver, Natural widths of atomic K and L levels, Kα X-ray lines and several KLL Auger lines, J. Phys. Chem. Ref. Data. 8 (1979) 329–338. doi:10.1063/1.555595.

[28] F. Dallavalle, G. Folesani, R. Marchelli, G. Galaverna, Stereoselective Formation of Ternary Copper(II) Complexes of (S)-amino-acid amides and (R)- or (S)-amino acids in aqueous solution, Helv. Chim. Acta. 77 (1994) 1623–1630. doi:10.1002/hlca.19940770619.

[29] P. Gans, A. Sabatini, A. Vacca, Investigation of equilibria in solution. Determination of equilibrium constants with the HYPERQUAD suite of programs, Talanta. 43 (1996) 1739–1753. doi:10.1016/0039-9140(96)01958-3.

[30] Z. Xiao, F. Loughlin, G.N. George, G.J. Howlett, A.G. Wedd, C-terminal domain of the membrane copper transporter Ctr1 from Saccharomyces cerevisiae binds four Cu(I) ions as a cuprous-thiolate polynuclear cluster: sub-femtomolar Cu(I) affinity of three proteins involved in copper trafficking., J. Am. Chem. Soc. 126 (2004) 3081–3090. doi:10.1021/ja0390350.

[31] K.Y. Djoko, L.X. Chong, A.G. Wedd, Z. Xiao, Reaction mechanisms of the multicopper oxidase CueO from Escherichia coli support its functional role as a cuprous oxidase, J. Am. Chem. Soc. 132 (2010) 2005–2015. doi:10.1021/ja9091903.

[32] Z. Xiao, J. Brose, S. Schimo, S.M. Ackland, S. La Fontaine, A.G. Wedd, Unification of the copper(I) binding affinities of the metallo-chaperones Atx1, Atox1, and related proteins: detection probes and affinity standards., J. Biol. Chem. 286 (2011) 11047–55. doi:10.1074/jbc.M110.213074.

[33] B. Alies, B. Badei, P. Faller, C. Hureau, Reevaluation of copper(I) affinity for amyloid-β peptides by competition with ferrozine-an unusual copper(I) indicator, Chem. Eur. J. 18 (2012) 1161–1167. doi:10.1002/chem.201102746.

[34] P. Kamau, R.B. Jordan, Complex formation constants for the aqueous copper(i)−acetonitrile system by a simple general method, Inorg. Chem. 40 (2001) 3879–3883. doi:10.1021/ic001447b.

[35] L. Alderighi, P. Gans, A. Ienco, D. Peters, A. Sabatini, A. Vacca, Hyperquad simulation and speciation (HySS): a utility program for the investigation of equilibria involving soluble and partially soluble species, Coord. Chem. Rev. 184 (1999) 311–318. doi:10.1016/S0010-8545(98)00260-4.

[36] L.S. Kau, D.J. Spira-Solomon, J.E. Penner-Hahn, K.O. Hodgson, E.I. Solomon, X-ray absorption edge determination of the oxidation state and coordination number of copper. Application to the type 3 site in Rhus vernicifera laccase and its reaction with oxygen, J. Am. Chem. Soc. 109 (1987) 6433–6442. doi:10.1021/ja00255a032.

[37] I.J. Pickering, G.N. George, C.T. Dameron, B. Kurz, D.R. Winge, I.G. Dance, X-ray absorption spectroscopy of cuprous-thiolate clusters in proteins and model systems, J. Am. Chem. Soc. 115 (1993) 9498–9505. doi:10.1021/ja00074a014.

[38] G. Aquilanti, M. Giorgetti, M. Minicucci, G. Papini, M. Pellei, M. Tegoni, A. Trasatti, C. Santini, A study on the coordinative versatility of new N,S-donor macrocyclic ligands: XAFS, and Cu^{2+} complexation thermodynamics in solution., Dalton Trans. 40 (2011) 2764–77. doi:10.1039/c0dt01401j.

[39] D.J. Darensbourg, J.B. Robertson, D.L. Larkins, J.H. Reibenspies, Water-soluble organometallic compounds. 7.1 further studies of 1,3,5-triaza-7-phosphaadamantane

derivatives of group 10 metals, including metal carbonyls and hydrides, Inorg. Chem. 38 (1999) 2473–2481. doi:10.1021/ic981243j.

[40] A. Filipponi, Statistical errors in X-ray absorption fine-structure data analysis, J. Phys. Condens. Matter. 7 (1995) 9343–9356. doi:10.1088/0953-8984/7/48/022.

[41] V. Gandin, F. Tisato, A. Dolmella, M. Pellei, C. Santini, M. Giorgetti, C. Marzano, M. Porchia, in vitro and in vivo anticancer activity of copper(I) complexes with homoscorpionate tridentate tris(pyrazolyl)borate and auxiliary monodentate phosphine ligands, J. Med. Chem. 57 (2014) 4745–4760. doi:10.1021/jm500279x.

[42] M. Benfatto, P. D'Angelo, S. Della Longa, N. V Pavel, Evidence of distorted fivefold coordination of the Cu^{2+} aqua ion from an X-ray-absorption spectroscopy quantitative analysis, Phys. Rev. B. 65 (2002) 174205. doi:10.1103/PhysRevB.65.174205.

[43] E. Maccaroni, H. Dong, O. Blacque, H.W. Schmalle, C.M. Frech, H. Berke, Water soluble phosphine rhenium complexes, J. Organomet. Chem. 695 (2010) 487–494. doi:10.1016/j.jorganchem.2009.11.031.

[44] C. Scolaro, A. Bergamo, L. Brescacin, R. Delfino, M. Cocchietto, G. Laurenczy, T.J. Geldbach, G. Sava, P.J. Dyson, In vitro and in vivo evaluation of ruthenium(II)−arene PTA complexes, J. Med. Chem. 48 (2005) 4161–4171. doi:10.1021/jm050015d.

[45] Z. Xiao, P.S. Donnelly, M. Zimmermann, A.G. Wedd, Transfer of copper between bis(thiosemicarbazone) ligands and intracellular copper-binding proteins. insights into mechanisms of copper uptake and hypoxia selectivity, Inorg. Chem. 47 (2008) 4338–4347. doi:10.1021/ic702440e.

[46] K.L. Haas, A.B. Putterman, D.R. White, D.J. Thiele, K.J. Franz, Model peptides provide new insights into the role of histidine residues as potential ligands in human cellular copper acquisition via Ctr1, J. Am. Chem. Soc. 133 (2011) 4427–37. doi:10.1021/ja108890c.

[47] L.A. Yatsunyk, A.C. Rosenzweig, Cu(I) binding and transfer by the N terminus of the wilson disease protein, J. Biol. Chem. 282 (2007) 8622–8631. doi:10.1074/jbc.M609533200.

[48] M. Porchia, F. Tisato, M. Zancato, V. Gandin, C. Marzano, In vitro antitumor activity of water-soluble copper(I) complexes with diimine and monodentate phosphine ligands, Arab. J. Chem. (2017). doi:10.1016/j.arabjc.2017.09.003.

[49] L.X. Chong, M.-R. Ash, M.J. Maher, M.G. Hinds, Z. Xiao, A.G. Wedd, Unprecedented binding cooperativity between Cu^{I} and Cu^{II} in the copper resistance protein CopK from Cupriavidus metallidurans CH34: implications from structural studies by NMR spectroscopy and X-ray crystallography, J. Am. Chem. Soc. 131 (2009) 3549–3564. doi:10.1021/ja807354z.

[50] R. Miras, I. Morin, O. Jacquin, M. Cuillel, F. Guillain, E. Mintz, Interplay between glutathione, Atx1 and copper. 1. Copper(I) glutathionate induced dimerization of Atx1, J. Biol. Inorg. Chem. 13 (2008) 195–205. doi:10.1007/s00775-007-0310-2.

[51] K.A. Wills, H.J. Mandujano-Ramirez, G. Merino, D. Mattia, T. Hewat, N. Robertson, G. Oskam, M.D. Jones, S.E. Lewis, P.J. Cameron, Investigation of a copper(I) biquinoline complex for application in dye-sensitized solar cells, RSC Adv. 3 (2013) 23361–23369. doi:10.1039/C3RA44936J.

[52] S.G. Aller, V.M. Unger, Projection structure of the human copper transporter CTR1 at 6-Å resolution reveals a compact trimer with a novel channel-like architecture, Proc. Natl. Acad. Sci. USA 103 (2006) 3627–3632. doi:10.1073/pnas.0509929103.

[53] C.J. De Feo, S.G. Aller, G.S. Siluvai, N.J. Blackburn, V.M. Unger, Three-dimensional structure of the human copper transporter hCTR1, Proc. Natl. Acad. Sci. USA 106 (2009) 4237–4242. doi:10.1073/pnas.0810286106.

[54] E. Atrián-Blasco, E. Cerrada, A. Conte-Daban, D. Testemale, P. Faller, M. Laguna, C. Hureau, Copper(I) targeting in the Alzheimer's disease context: a first example using the biocompatible PTA ligand, Metallomics. 7 (2015) 1229–1232. doi:10.1039/C5MT00077G.

[55] M. Tegoni, D. Valensin, L. Toso, M. Remelli, Copper chelators: chemical properties and bio-medical applications, Curr. Med. Chem. 21 (2014) 3785–3818. doi:10.2174/09298673216661406011619 39.